

Synthesis, Intramolecular Hydrogen Bonding and Conformation of Optically Active Bilirubin Amides. Analysis by Circular Dichroism and NMR

Stefan E. Boiadjiev, Richard V. Person and David A. Lightner*

Department of Chemistry, University of Nevada
Reno, Nevada 89557-0020 USA

(Received in UK 17 December 1992)

Abstract: The conformation of the diamide and the bis-N-methylamide of an optically active analog of bilirubin ($\beta S, \beta' S$ -dimethylmesobilirubin-XIII α) is stabilized in a ridge-tile shape by intramolecular hydrogen bonding, as detected by $^1\text{H-NMR}$ and CD spectroscopy. The matrix of intramolecular hydrogen bonds resists disruption even in $(\text{CH}_3)_2\text{SO}$ solvent, where very strong exciton coupling CD is evident: $\Delta\epsilon_{427}^{\text{max}} -417$, $\Delta\epsilon_{383}^{\text{max}} +234$ (diamide).

INTRODUCTION

Bilirubin-IX α (Fig. 1), the yellow-orange neurotoxic pigment of jaundice, is formed in human metabolism by the normal turnover of hemoglobin and other heme proteins.¹⁻³ It is a conformationally mobile bichromophore with characteristics of a molecular propeller. Rotation of the dipyrinone chromophores about the central $-\text{CH}_2-$ unit at C_{10} generates a large number of conformational isomers, of which a ridge-tile shape conformer has a minimum number of non-bonded steric interactions.³⁻⁵ This is also a conformation that brings the two propionic acid groups (located at C_8 and C_{12}) into close proximity with the pyrrole N-H and lactam $-\text{NH}-\text{C}=\text{O}$ groups, with the result that a network of intramolecular hydrogen bonds can easily be established — thus rendering the ridge-tile conformation unusually stable.⁶ This inward tucking of the CO_2H groups and tethering to opposing dipyrinones through intramolecular hydrogen bonding also lowers the acidity and decreases the polarity of the pigment, leaving it unexcretable in normal metabolism (hepatic excretion), except *via* glucuronidation. The ridge-tile conformation is found in crystalline bilirubin and its salts,^{7,8} and it is favored by bilirubin in non-polar organic solvents,⁹⁻¹¹ and

Dedicated to the late Professor Dr. Günther Snatzke (deceased January 14, 1992)

even in polar solvents.^{9,11} However, when the propionic acid groups are translocated away from C₈ and C₁₂, the solution properties of the pigment undergo significant changes. Such pigments are more polar than bilirubin and much less soluble in non-polar organic solvents, such as chloroform,¹² and they typically are more excretable (hepatic excretion), usually not requiring glucuronidation.^{13,14} However, analogs with propionic acid groups at C₈ and C₁₂, *e.g.* mesobilirubin-XIII α (Fig. 1) typically share the unique (non) polarity and (non) excreatability properties as bilirubin. For these pigments, like bilirubin have their CO₂H groups sequestered through intramolecular hydrogen bonding.

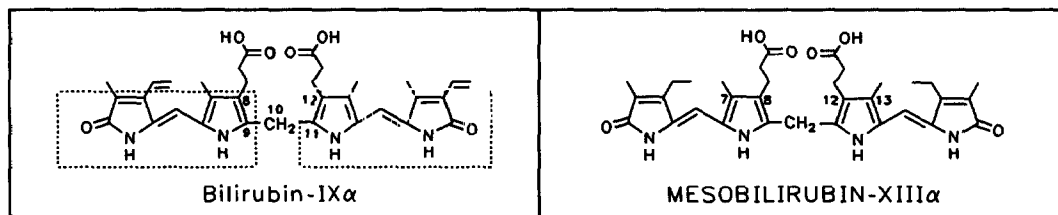


FIGURE 1. (Left) Bilirubin-IX α with its two dipyrri-2,4-dione chromophores shown enclosed in dashed boxes. (Right) Mesobilirubin-XIII α , a symmetric analog of bilirubin-IX α , with ethyl groups.

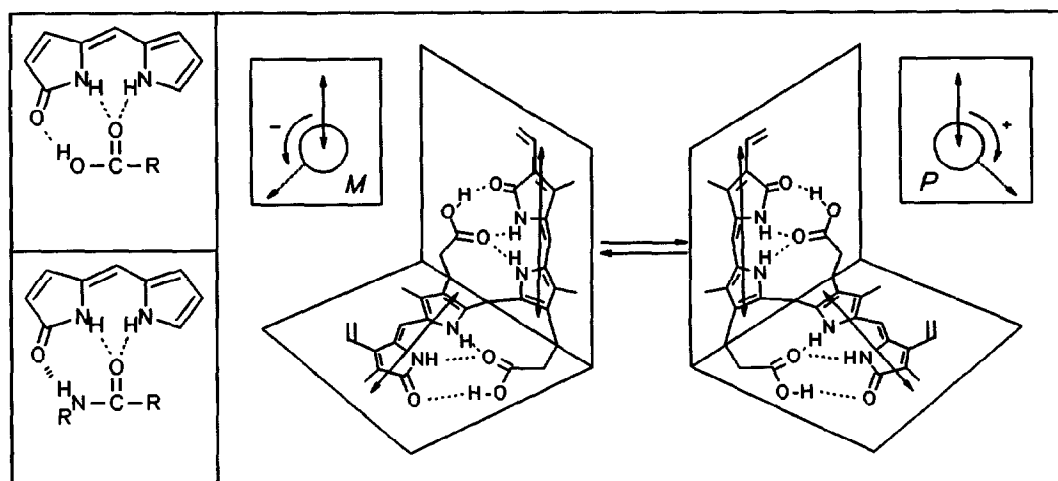
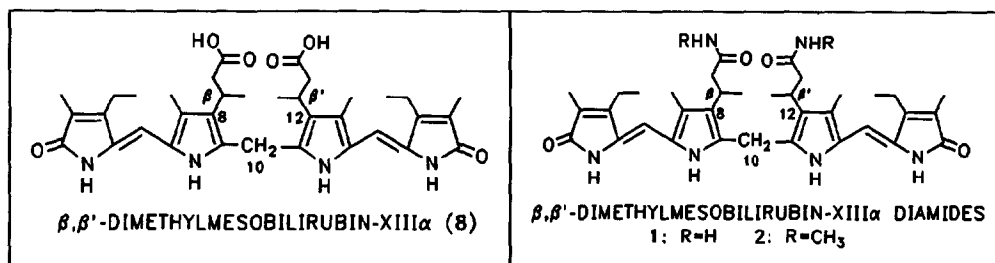


FIGURE 2. (Left) Partial structure showing a dipyrri-2,4-dione fragment hydrogen bonded to a carboxylic acid group (upper) and to an amide group (lower). (Right) Interconverting intramolecularly hydrogen-bonded enantiomeric conformers of bilirubin-IX α . The double headed arrows represent the dipyrri-2,4-dione chromophore long wavelength electric transition moment vectors (dipoles). The relative helicities (*M*, minus or *P*, plus) of the vectors are shown (inset) for each enantiomer.

Bilirubin intramolecular hydrogen bonding (Fig. 2) is one of the most interesting and important facets of bilirubin conformation.^{3,7,9,10,15} Although the two component dipyrri-2,4-dione units of bilirubin-type molecules may rotate relatively freely and independently about the interconnecting central -CH₂- group,

two non-superimposable mirror image conformations are uniquely stabilized through an extensive network of intramolecular hydrogen bonds. These conformational enantiomers are known to interconvert fairly rapidly at room temperature over a barrier of ~ 20 kcal/mole.^{9,10} Our interest in stabilization of pigment stereochemistry through the action of intramolecular hydrogen bonding led us to consider: (1) whether such hydrogen bonding might be retained in a bilirubin analog where both propionic acid groups are replaced by propionamide groups, and (2) how such hydrogen bonding might affect the conformation of the pigment.

For this study we chose mesobilirubin-XIII α as a model for bilirubin. In particular we chose mesobilirubin-XIII α models with one methyl group at each β -position of the two propionic acid side chains, thereby creating potentially optically active isomers [($\beta S, \beta' S$) and ($\beta R, \beta' R$)] for use in probing pigment stereochemistry through circular dichroism spectroscopy. As will be illustrated, the β -methyl groups perturb the equilibrium depicted in Fig. 2 through non-bonded steric interactions (with C₁₀ hydrogens), with the result that the equilibrium is shifted toward the *M*-chirality conformer in the $\beta S, \beta' S$ enantiomer — and shifted toward the *P*-chirality conformer in the ($\beta R, \beta' R$) enantiomer.¹⁶ The equilibrium displacement, however, obtains only in intramolecularly hydrogen-bonded conformers. Thus these optically active pigments can be viewed as powerful chiral probes of pigment stereochemistry and intramolecular hydrogen bonding. In the following we report on the synthesis, spectroscopic properties and conformational analysis of the bis-amide (1) and bis-*N*-methylamide (2) of β, β' -dimethylmesobilirubin-XIII α (8).

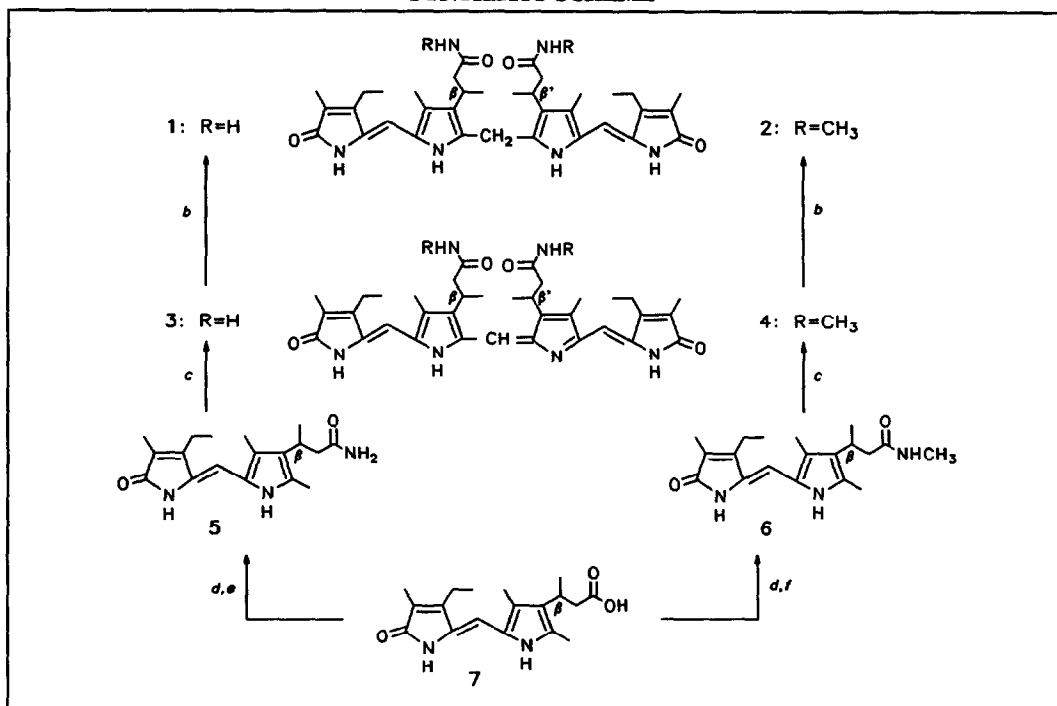


RESULTS AND DISCUSSION

Synthesis. The target amides (1 and 2) were obtained through the series of steps outlined in the Synthetic Scheme. A more direct route would have involved reaction of the appropriate stereoisomer(s) of β, β' -dimethylmesobilirubin (8)¹⁶ in the Shioiri reaction,¹⁷⁻¹⁹ which involves activation of the carboxylic acid groups with diphenylphosphoryl azide in dry dimethylformamide (DMF) followed by reaction with the appropriate amine hydrochloride in the presence of triethylamine. Although this approach was successful with mesobilirubin-XIII itself, we could not induce its β, β' -dimethyl analog (8) to react satisfactorily. Consequently, we prepared dipyrnone amides 5 and 6 from 7 and subjected them to the oxidative coupling using *p*-chloranil in the presence of hot 98% formic acid²⁰ to give the corresponding verdins (3 and

4) as blue needles in 44-63% yield. Reduction of the verdins using sodium borohydride in tetrahydrofuran-methanol solvent afforded the corresponding bright yellow mesobilirubin amides (1 and 2) in 39-80% yield. The reaction sequence, when carried out with racemic dipyrinone amides, afforded a mixture of racemic [($\beta S, \beta' S$) + ($\beta R, \beta' R$)] and meso ($\beta S, \beta' R$) diastereomers of verdins and rubins. We were unable to separate the diastereomers of the bis-*N*-methylamides (2) and the primary amides (1); however, the pure rubin and verdin enantiomers, ($\beta S, \beta' S$) or ($\beta R, \beta' R$), could be synthesized from enantiomerically pure or highly enriched (βS) or (βR) dipyrinone acids (7a or 7b), which were available from an earlier study.¹⁶

SYNTHETIC SCHEME^a

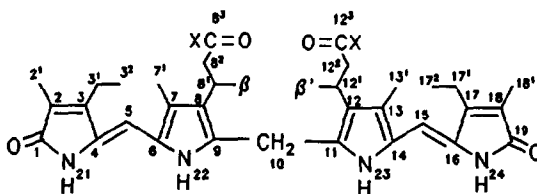


^a The a series has the (βS)-configuration, the b series has the (βR)-configuration; ^b NaBH₄; ^c chloranil/HCO₂H/reflux; ^d Diphenylphosphoryl azide/DMF/(CH₃CH₂)₃N; ^e NH₄Cl; ^f CH₃NH₃Cl.

NMR Analysis and Intramolecular Hydrogen Bonding. Intramolecular hydrogen bonding is believed to be the most important factor in stabilizing the folded, ridge-tile conformation of bilirubin in the crystal^{3,7} and in solution in non-polar solvents.^{3,9,10,21} It is thought to be important even in polar and hydroxylic solvents,^{3,9c,22} and it is of major importance to the success of the allosteric model essential to this work. The potential for intramolecular hydrogen bonding in the primary and secondary amides of mesobilirubin differs little from that of the parent acid, as in Fig. 2 with NH replacing OH. Such hydrogen bonding can

often be detected by $^1\text{H-NMR}$ spectroscopy, especially in non-polar solvents.^{9d} The $^1\text{H-NMR}$ data (Table 1) for **1a** and **2a** may be compared with those of the parent acid (**8a**): significantly, the proton chemical shifts are very similar. Of special importance are the lactam and pyrrole N-H chemical shifts in CDCl_3 , a solvent in which intramolecular hydrogen bonding has previously been established for bilirubins.^{9,21} The strongly deshielded lactam N-H chemical shifts suggest the presence of hydrogen bonding to the propionic carbonyl, and the relatively more shielded pyrrole N-H chemical shifts are a strong indication of a folded conformation, as depicted in Fig. 2, where one pyrrole N-H lies above the π -system of the other. Just as the strongly deshielded acid OH confirms its hydrogen bonding (to the lactam C=O), the strongly deshielded propionamide N-H resonances of **1a** and **2a** imply participation in hydrogen bonding. Noteworthy is

TABLE 1. Proton NMR Spectra (δ , ppm downfield from $(\text{CH}_3)_4\text{Si}$) of the ($\beta\text{S},\beta'\text{S}$) Enantiomers β,β' -Dimethylmesobilirubin-XIII α (**8a**), Diamide (**1a**) and Bis-N-methylamide (**2a**) in CDCl_3 and $(\text{CD}_3)_2\text{SO}$ at 22°C.



Type	Site	δ in CDCl_3			δ in $(\text{CD}_3)_2\text{SO}$		
		8a (X=OH)	1a (X=NH ₂)	2a (X=NHCH ₃)	8a (X=OH)	1a (X=NH ₂)	2a (X=NHCH ₃)
COOH or CONHR	8 ³ ,12 ³	13.60(s)	8.91(brs) 5.55(brs)	8.92(brq) ^j	11.98(brs)	8.24(brs) 8.22(brs)	8.30(brq) ^r
NH	21,24	10.68(s)	10.77(brs)	11.04(brs)	9.85(brs)	9.90(s)	10.05(brs)
NH	22,23	9.04(s)	9.88(brs)	10.13(brs)	10.10(brs)	10.94(s)	10.25(brs)
CH ₃	β,β'	1.35(d) ^a	1.29(d) ^f	1.34(d) ^f	0.98(d) ^m	1.22(d) ^m	1.16(d) ^m
CH	8 ¹ ,12 ¹	3.45(ddq) ^b	3.52(ddq) ^g	3.55(ddq) ^g	3.17(dq) ⁿ	3.42(m)	3.39(m)
CH ₂	8 ² ,12 ²	2.70(dd) ^c 3.08(dd) ^d	2.62(dd) ^h 2.89(dd) ⁱ	2.47(dd) ^k 3.09(dd) ^l	2.40(dd) ^o	2.60(dd) ^p 2.93(dd) ^q	2.63(dd) ^f
CH ₃	7 ¹ ,13 ¹	2.24(s)	2.21(s)	2.24(s)	2.08(s)	2.19(s)	2.13(s)
CH ₂	3 ¹ ,17 ¹	2.48(q) ^e	2.47(q) ^e	2.48(q) ^e	2.44(q) ^a	2.48(q) ^a	2.48(q) ^a
CH ₃	3 ² ,17 ²	1.11(t) ^e	1.12(t) ^e	1.11(t) ^e	1.07(t) ^a	1.04(t) ^a	1.06(t) ^a
CH ₃	2 ¹ ,18 ¹	1.85(s)	1.82(s)	1.85(s)	1.76(s)	1.73(s)	1.73(s)
=CH	5,15	6.04(s)	5.96(s)	5.96(s)	5.95(s)	5.99(s)	5.92(s)
-CH ₂ -	10	4.06(s)	4.01(s)	4.03(s)	3.98(s)	3.91(s)	3.90(s)
NCH ₃	8 ⁵	—	—	2.90(d) ^j	—	—	2.50(d) ^r

^aJ=7.4 Hz; ^bJ=3.0, 12.0, 7.4 Hz; ^cJ=3.0, 18.2 Hz; ^dJ=12.3, 18.2 Hz; ^eJ=7.6 Hz; ^fJ=7.3 Hz;

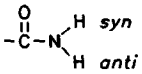
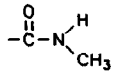
^gJ=3.5, 11.7, 7.3 Hz; ^hJ=3.2, 16.9 Hz; ⁱJ=12.1, 16.9 Hz; ^jJ=5.0 Hz; ^kJ=2.6, 17.5 Hz;

^lJ=11.9, 17.5 Hz; ^mJ=7.0 Hz; ⁿJ=8.8, 7.1 Hz; ^oJ=8.7, 8.1 Hz; ^pJ=3.0, 16.2 Hz; ^qJ=12.6, 16.2 Hz;

^rJ=4.5 Hz; ^sJ=10.8 Hz, overlapped.

the large difference in chemical shifts of the two propionamide *N-H* resonances of **1a**. We attribute the more deshielded resonance to the *syn-H* involved in hydrogen bonding — and the more shielded resonance to the *anti-H* (not involved). This large difference stands in contrast to the ordinary behavior of propionamide *N-H*s, as seen in dipyrinone **5a** in CDCl_3 (Table 2). Those data strongly implicate one of the propionamide *N-H*s in hydrogen bonding and support the thesis that intramolecularly hydrogen bonded structures (akin to Fig. 2) are involved. In $(\text{CD}_3)_2\text{SO}$, a solvent known to hydrogen bond to OH and NH residues,^{3,21,23} the CO_2H resonance is more strongly shifted (upfield) than the *N-H* resonances from the CONH group, suggesting a greater solvent perturbation on the intramolecular hydrogen bonding matrix (of Fig. 2).

TABLE 2. Comparison of $^1\text{H-NMR}$ Chemical Shifts of Amide *N-H* and *N-CH*₃ Resonances in Dipyrinones and Mesobilirubins in CDCl_3 and $(\text{CD}_3)_2\text{SO}$ Solvent at 22°C.

								
ppm	1a	5a	1a^a	5a^a	2a	6a	2a^a	6a^a
δ_{syn}	8.91	5.54	8.24	7.23	8.91	5.28	8.30	7.66
δ_{anti}	5.55	5.33	8.22	6.65	2.91 ^b	2.71 ^b	2.50 ^b	2.48 ^b
$\Delta\delta$ (NH)	3.36	0.21	0.02	0.58	—	—	—	—

^a In $(\text{CD}_3)_2\text{SO}$ solvent. ^b CH_3 signal.

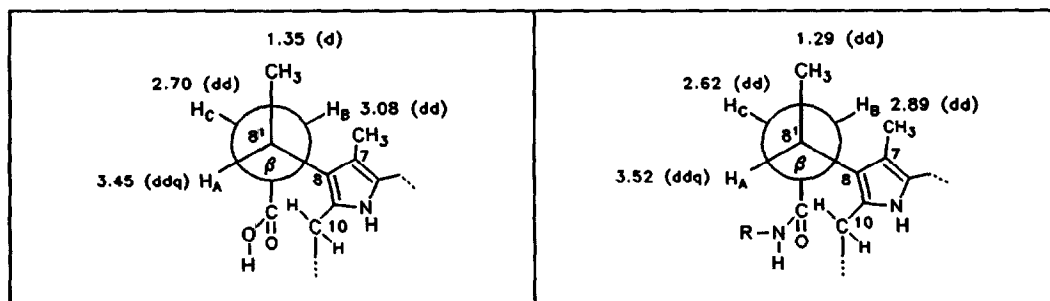


FIGURE 3. Newman projections for the propionic acid residues in $(\beta S, \beta' S)$ -dimethylmesobilirubin-XIII α (**8a**) (Left) and in its diamide (**1a**, $\text{R}=\text{H}$) or bis-*N*-methylamide (**2a**, $\text{R}=\text{CH}_3$) (Right). The chemical shifts and splittings are assigned to the relevant protons on the basis of earlier assignments for **8a** (ref. 16) bilirubin (ref. 9b).

Further support for a stable, intramolecularly hydrogen-bonded ridge-tile conformation comes from analysis of vicinal H | H coupling in the propionic acid or amide side chains. Confirming a molecular shape where the propionic residues are constrained to adopt fixed conformations, vicinal H | H coupling constants (**8a** : $J_{\text{AC}}=3$ Hz, $J_{\text{AB}}=12$ Hz; and mesobilirubin-XIII α : $J_{\text{AC}}=3$ Hz, $J_{\text{AB}}=13$ Hz) in the

propionic acid segments, $-\text{CH}_A(\text{CH}_3)-\text{CH}_B\text{H}_C-\text{CO}_2\text{H}$ and $-\text{CH}_A\text{H}_X-\text{CH}_B\text{H}_C-\text{CO}_2\text{H}$, respectively) are not the averaged values seen in flexible chains (*cf* data in $(\text{CD}_3)_2\text{SO}$: $J_{AC}=J_{AB} \approx 8$ Hz). The data are consistent with a fixed and staggered segment geometry (Fig. 3) with an $\text{H}_A-\text{C}-\text{C}-\text{H}_C$ torsion angle of $\sim 60^\circ$ and an $\text{H}_A-\text{C}-\text{C}-\text{H}_B$ torsion angle of $\sim 180^\circ$ — close to the geometry seen in Dreiding models or in the global energy minimum conformation.¹⁶ Also importantly, they indicate that the conformational enantiomerism depicted in Fig. 2 is slow on the NMR time scale.^{9,10}

Conformational Analysis from Molecular Dynamics Calculations. Molecular dynamics calculations on bilirubin confirm the importance of intramolecular hydrogen bonding. The conformational energy map (Fig. 4) for rotations of the dipyrinones about C_{10} reveals a collection of isoenergetic global minima, which correspond to either identical or mirror image structures represented by the *M* and *P* chirality conformers shown. Interestingly, aside from differences due to enantiomerism, the global energy minimum conformation of bilirubin is essentially the same, whether hydrogen bonding is present or absent. Thus, with full hydrogen bonding the global energy minimum for the *P*-chirality conformer lies at $\phi_1 = \phi_2 \approx 63^\circ$; in the absence of hydrogen bonding it lies at $\phi_1 = \phi_2 \approx 70^\circ$. However, the stabilization due to intramolecular hydrogen bonding is potentially considerable, which we compute to be ~ 20 kcal/mole. This suggests that other conformers are essentially absent and that studies of bilirubin conformation should, as a starting point, focus on intramolecularly hydrogen-bonded structures.

The "internal" stereochemistry and non-bonded steric interactions in the intramolecularly-bonded conformers is quite revealing. Close inspection of the steric environment of each of the diastereotopic hydrogens in the $-\text{CH}_2-\text{CH}_2-$ fragment of the intramolecularly hydrogen-bonded propionic acid groups suggests a way to displace the *M* \rightleftharpoons *P* equilibrium of Fig. 4. Thus, when folded into the *M*-chirality ridge-tile enantiomer, the (*pro-R*)- β -hydrogen (but not the *pro-S*) is brought into close non-bonded contact with the central $-\text{CH}_2-$ group at C_{10} . On the other hand, in the *P*-chirality enantiomer, it is the (*pro-S*)- β -hydrogen that is buttressed against the $\text{C}_{10}-\text{CH}_2-$ group. Consequently, when bilirubin-IX (or mesobilirubin-XIII α) adopts either of the thermodynamically preferred intramolecularly hydrogen bonded ridge-tile conformations, one conformational enantiomer is expected to be destabilized relative to the other through allosteric action by judicious replacement of hydrogens on the propionic acid chain by methyl groups. In earlier work,¹⁶ we showed that insertion of a methyl group at the *pro-S* site on the β -carbon of the mesobilirubin-XIII α (Fig. 1) propionic acid shifts the conformational equilibrium toward *M* by destabilizing the *P*-chirality intramolecularly hydrogen-bonded conformational enantiomer through the introduction of a severe non-bonded $\text{CH}_3 | \text{CH}_2$ steric interaction with the $\text{C}_{10}-\text{CH}_2-$ group. Alternatively, introduction of a methyl group at the *pro-R* site destabilizes the *M*-chirality enantiomer and shifts the equilibrium toward *P*. Assuming that intramolecular hydrogen bonding remains a potent conformation-stabilizing force, introduction of such methyl groups might thus be expected to force the resolution of mesobilirubin

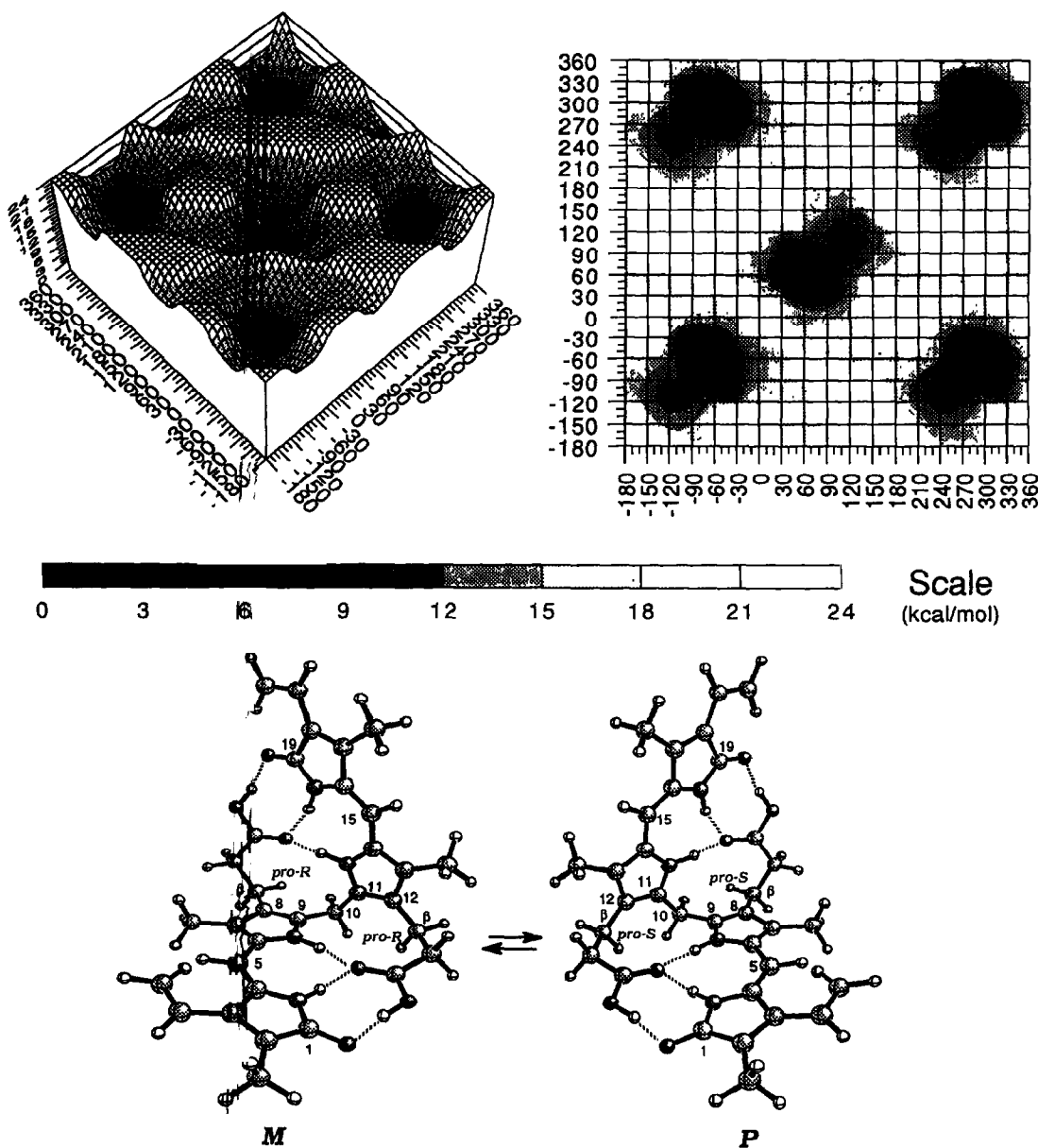


FIGURE 4. (Upper Left) Potential energy surface and (Upper Right) contour map for bilirubin-IX α conformations generated by rotating the two dipyrinone groups independently about the C₉-C₁₀ and C₁₀-C₁₁ bonds (ϕ_1 and ϕ_2 respectively). The energy scale (Middle) is in kcal/mol, and global minima (set to 0 kcal/mol) are found near $(\phi_1, \phi_2) \approx (60^\circ, 60^\circ)$ (*P*-chirality), and $(\phi_1, \phi_2) \approx (-60^\circ, -60^\circ)$, $(-60^\circ, 300^\circ)$, $(300^\circ, -60^\circ)$, $(300^\circ, 300^\circ)$ (*M*-chirality). Data are from molecular dynamics simulations using SYBYL[®] (Tripos Assoc.) on an Evans & Sutherland ESV-10 workstation. (Lower) Ball and stick conformational representations for the ridge-tilt shape *M* and *P*-chirality intramolecularly hydrogen bonded, interconverting enantiomers of bilirubin-IX α . In the propionic acid side chains attached to pyrrole ring carbons C₈ and C₁₂, the hydrogens on the β and β' -CH₂- groups are either *pro-R* or *pro-S* (only one hydrogen of the set is designated). When the *M*-chirality conformer inverts into the *P*-chirality, steric crowding of the *pro-R* hydrogens is relieved and replaced by similar crowding of the *pro-S* hydrogens. Drawings from Müller and Falk's "Ball and Stick" program (Cherwell Scientific, Oxford, U.K.) for the Macintosh.

amides through intramolecular steric interactions.

The experimental evidence for intramolecular hydrogen bonding in **1a** and **2a** is fully supported by molecular dynamics calculations, which show global energy minima for $\beta S, \beta' S$ near $(\phi_1 = \phi_2 \approx -60^\circ)$, $(\phi_1 \approx -60^\circ, \phi_2 \approx 300^\circ)$, $(\phi_1 \approx 300^\circ, \phi_2 \approx -60^\circ)$ and $(\phi_1 = \phi_2 \approx 300^\circ)$, corresponding to the *M*-chirality conformer of Fig. 5. A local minimum corresponding to the *P*-chirality conformer is found near $(\phi_1 = \phi_2 \approx 60^\circ)$ and lies some 4.5 kcal/mole higher in energy than the *M*-chirality due to non-bonded steric interactions between the β -methyls and the C_{10} -CH₂-. Intramolecular hydrogen bonding remains an important factor despite the non-bonded steric interaction, but one conformational diastereomer (*M*) is clearly favored over the other (*P*). Secondary, higher energy local minima can also be detected. Four isoenergetic local minima $[(\phi_1 = \phi_2 \approx -110^\circ)$, $(\phi_1 \approx -110^\circ, \phi_2 \approx 250^\circ)$, $(\phi_1 = \phi_2 \approx 250^\circ)$ and $(\phi_1 \approx 250^\circ, \phi_2 \approx -110^\circ)]$ lie some 9-10 kcal/mole higher in energy than the nearby *M*-chirality global minima. A corresponding local minimum $(\phi_1 = \phi_2 \approx 115^\circ)$ located nearby the *P*-chirality minimum at $(\phi_1 = \phi_2 \approx 60^\circ)$ lies some 7-8 kcal/mole above the global minimum, *M*. In these secondary local minima, residual hydrogen bonding is still maintained; however, in view of the predicted large energy difference between these secondary local minima and an *M*-chirality global minimum, they may be expected to contribute very little to the conformation of **1a** and **2a**. Similarly, on the basis of energy considerations the *P*-chirality conformer of **1a** probably contributes little to the overall conformation population.

Nuclear Overhauser Effect. The conclusions reached above on the conformation of **1a** and **2a** are supported additionally by ¹H-NMR NOE measurements. In the most stable *M*-chirality conformation (Fig. 5, upper left) of **1a** or **2a** (or *P*-chirality conformation of **1b** or **2b**) the C_{10} -CH₂- lies close to the β, β' -hydrogens at C_8^1 and C_{12}^1 and distant from the β, β' -methyl groups at C_8^1 and C_{12}^1 . One might therefore expect to see a strong NOE between the C_{10} -CH₂- hydrogens and the β, β' -hydrogens, but no NOE, or at best a very weak NOE, for the β, β' -methyls. The β, β' methine hydrogens at C_8^1 and C_{12}^1 (3.52 ppm in **1a** and 3.55 ppm in **2a**, Table 1) show a strong NOE on the C_{10} -CH₂- hydrogens (at 4.01 ppm in **1a** and 4.03 ppm in **2a**) but no NOE on the pyrrole ring methyls at C_7 and C_{13} (2.21 ppm in **1a** and 2.24 ppm in **2a**). In contrast, the β -methyls at C_8^1 and C_{12}^1 (1.29 ppm in **1a** and 1.34 ppm in **2a**) show strong NOEs on the pyrrole ring methyls at C_7^1 and C_{13}^1 but no NOEs on the C_{10} -CH₂- group. These results are best accommodated by the intramolecularly hydrogen-bonded *M*-chirality conformation shown in Fig. 5. In further support of this stereochemistry, NOEs (weak) are found between H_B (but not H_C) and the propionamide *anti*-NH or CH₃N of **1a** and **2a**, respectively (see Table 2 and Fig. 3). Other strong NOEs found between (i) the lactam and pyrrole NHs, (ii) the hydrogens at C_5 and C_{15} and the ethyl hydrogens at C_3 and C_{17} , and (iii) the C_5/C_{15} hydrogens and the methyls at C_7 and C_{13} confirm that the dipyrinones of **1a** and **2a** adopt a *syn-Z* conformation, as shown. The parent ($\beta S, \beta' S$)-dimethylmesobilirubin (**8a**) shows similar NOEs, as reported previously.¹⁶

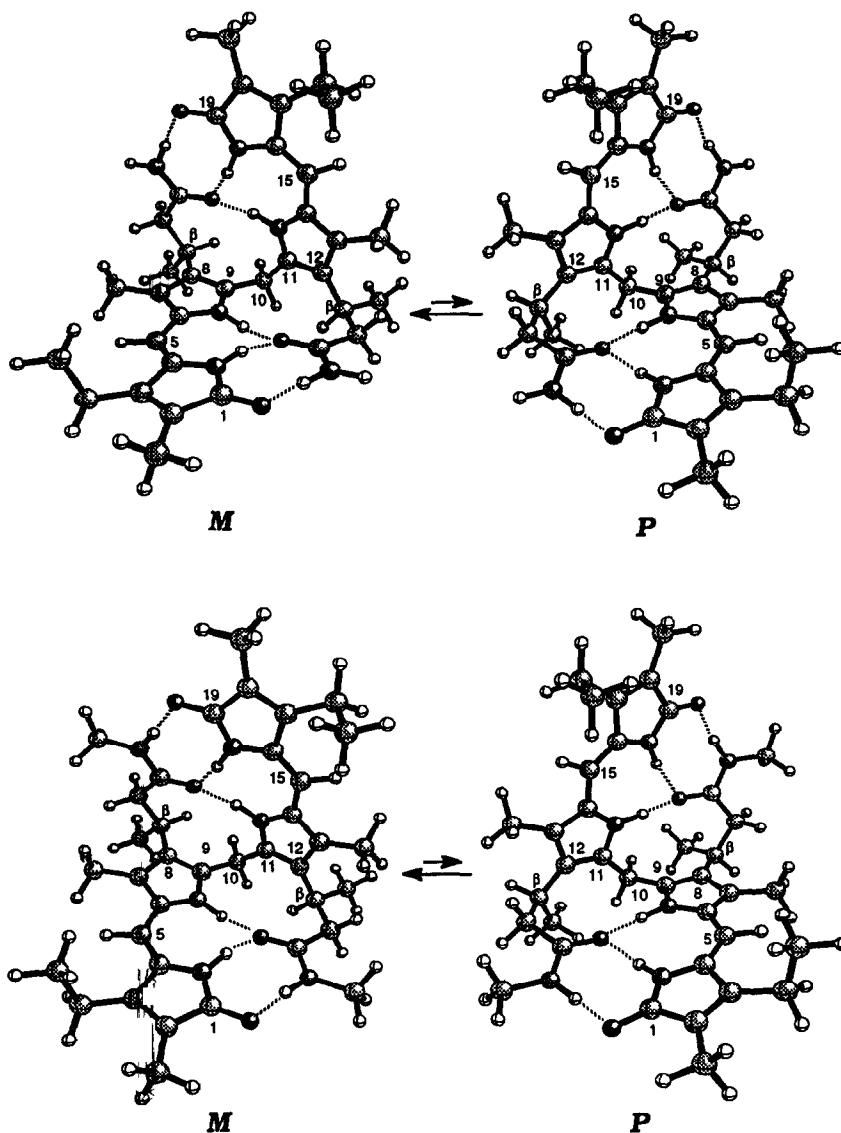


FIGURE 5. Ball and stick representations for the most stable conformations of (Upper) ($\beta S, \beta' S$)-dimethylmesobilirubin-XIII α amide (1a) and (Lower) ($\beta S, \beta' S$)-dimethylmesobilirubin-XIII α bis-N-methylamide (2a) in their ridge-tile shape. *M* and *P*-chirality intramolecularly hydrogen-bonded diastereomers. In the *M*-chirality diastereomer of 1a and 2a, the $\beta S, \beta' S$ methyl groups lie away from the C_{10} - CH_2 - group, but in the less stable (4.3 kcal higher energy) *P*-chirality diastereomer the methyls are buttressed against the C_{10} - CH_2 -.

Stereochemistry, Conformational Analysis and Circular Dichroism. With the introduction of chiral centers on the propionic side chains, as in the ($\beta S, \beta' S$)-dimethyl enantiomers of **1**, **2** and **8**, one can expect, at a minimum, modest optical activity from a π - π^* excitation in the dipyrinone perturbed by dissymmetric vicinal action. However, if intramolecular hydrogen bonding prevails, the conformational enantiomerism shown in Figs. 4 and 5 may be driven in either direction by equilibrium-displacing perturbations of an intramolecular origin, e.g., methyl substitution. If the predicted forced displacement of the $M \rightleftharpoons P$ equilibrium is achieved, then the two dipyrinone chromophores will be held in a fixed chiral geometry (M or P), depending on the R, S stereochemistry at β and β' ; and a strong exciton chirality^{4,24} interaction between them should lead to strong optical activity. Detection of optical activity (and an excess of the M or P chirality conformer) has been accomplished by circular dichroism (CD) spectroscopy on the parent acid enantiomers (**8a** and **8b**), which are found to exhibit very large bisignate Cotton effects (CEs), with $\Delta\epsilon$ values in the range 200–400 $M^{-1} \text{ cm}^{-1}$ for the pure enantiomers.¹⁶ Intense bisignate CD CEs are also seen (Fig. 6) for the primary and secondary bis-amides, **1a** and **2a** of ($\beta S, \beta' S$)-dimethylmesobilirubin (**8a**) — in complete agreement with the predictions of the allosteric model and exciton coupling theory.²⁴ As shown for a wide range of solvents (Table 3), the S, S -enantiomer of β, β' -dimethylmesobilirubin-XIII α (**8a**) and amides (**1a** and **2a**) with propionamide N-H groups show intense bisignate CDs that are characteristic of the M -helicity conformation. Data for the $\beta R, \beta' R$ enantiomers (not shown) give an equally intense bisignate CDs characteristic of the P -helicity conformer. Interestingly, the CE intensities for **1a** are very large, larger even than those of **2a** or **8a**, and the CD spectra are essentially invariant over a wide range of solvent polarity. Whether in a non-polar solvent or a polar, hydroxylic solvent, the CD intensity is either invariant (**1a**) or only slightly decreased (**2a** and **8a**), implying nearly the same enantioselectivity in both solvent types and very little loosening or disruption of the intramolecular hydrogen bonding network. The $\Delta\epsilon$ values in non-polar solvents like CHCl_3 are close to the theoretically predicted maximum values,²⁵ and not very different from the $\Delta\epsilon$ averaged over a wide range of organic solvents, excluding $(\text{CH}_3)_2\text{SO}$. One might expect the intramolecular hydrogen bonding, which is clearly so very important in stabilizing the M -chirality conformation of **1a**, **2a** and **8a** (and the P -chirality conformation of **1b**, **2b** and **8b**) to be strongest in non-polar solvents such as chloroform or diethyl ether, and weaker in polar aprotic solvents such as acetonitrile or acetone. Yet, the CD intensities in those solvents are within 10% of the average $\Delta\epsilon$ values. Apparently, there is very little influence from the polar solvent in disrupting the intramolecular hydrogen bonding network.

The CD behavior in $(\text{CH}_3)_2\text{SO}$ solvent is unique (Fig. 6). The CEs for the parent acid (**8a**) are substantially reduced, and the signs are reversed — consistent with a picture, proposed by Navon *et al.*^{9c} where the propionic residues are dissociated from hydrogen bonding to the dipyrinones yet still linked to them through solvent molecules.²³ In contrast, the CD of primary amide **1a** is the same as in all the

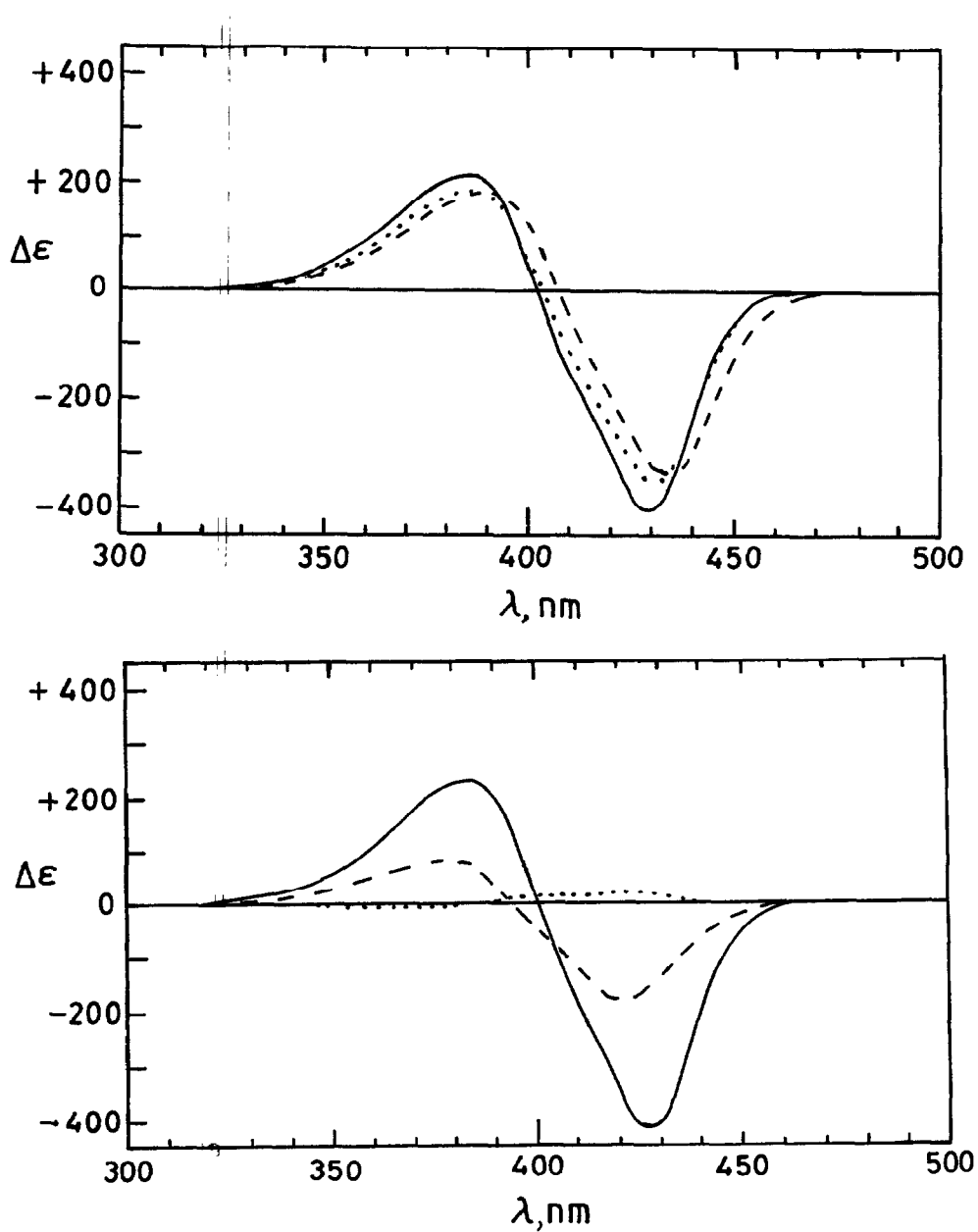


FIGURE 6. Circular dichroism spectra of $5 \times 10^{-5} M$ diamide 1a (—) and bis-N-methylamide 2a (---) of $(\beta S, \beta' S)$ -dimethylmesobilirubin-XIII α (8a) (\cdots) in (Upper) CHCl_3 and (Lower) $(\text{CH}_3)_2\text{SO}$ at 22°C .

TABLE 3. Circular Dichroism and Ultraviolet-Visible Spectral Data from $5 \times 10^{-5} M$ of Diamide 1a and Bis-N-methylamide 2a of ($\beta S, \beta' S$)-Dimethylmesobilirubin-XIII α (8a) at 22°C.

Pigment	Solvent	Dielectric Center	CD			UV	
			$\Delta\epsilon^{\max}(\lambda_1)$	λ_2 at $\Delta\epsilon=0$	$\Delta\epsilon^{\max}(\lambda_3)$	ϵ^{\max}	$\lambda(\text{nm})$
1a	Carbon tetrachloride	2.2	+178 (388)	400	-436 (430)	60,600	435
2a			+161 (391)	403	-410 (432)	57,600	435
8a			+179 (392)	406	-393 (434)	59,000	435
1a	Dioxane	2.2	+214 (384)	399	-435 (426)	62,200	426
2a			+172 (381)	398	-339 (426)	58,000	422
8a			+184 (389)	405	-336 (433)	56,600	431
1a	Benzene	2.3	+215 (386)	401	-454 (428)	62,600	430
2a			+186 (387)	402	-403 (430)	58,000	430
8a			+191 (390)	406	-362 (434)	55,400	433
1a	Toluene	2.4	+207 (387)	401	-444 (428)	59,100	430
2a			+178 (387)	402	-403 (430)	56,500	431
8a			+196 (391)	406	-375 (434)	55,800	433
1a	Diethyl Ether	4.3	+204 (384)	396	-462 (424)	65,700	425
2a			+168 (381)	397	-371 (424)	59,200	424
8a			+183 (387)	402	-365 (429)	57,500	429
1a	Chloroform	4.7	+216 (385)	402	-403 (429)	59,900	429
2a			+187 (386)	403	-348 (431)	57,600	428
8a			+186 (389)	407	-337 (434)	55,500	431
1a	Tetrahydrofuran	7.3	+217 (385)	399	-446 (427)	63,400	428
2a			+170 (382)	399	-339 (427)	57,200	423
8a			+188 (390)	406	-338 (433)	56,200	431
1a	Dichloromethane	8.9	+216 (383)	400	-395 (426)	60,600	428
2a			+182 (383)	400	-340 (427)	58,100	423
8a			+180 (392)	407	-319 (433)	54,800	431
1a	1,2-Dichloroethane	10.4	+220 (384)	400	-402 (426)	59,700	425
2a			+194 (383)	400	-359 (427)	57,000	423
8a			+193 (389)	407	-332 (433)	55,400	430
1a	1-Butanol	17.1	+247 (390)	406	-437 (434)	61,600	432
2a			+169 (387)	404	-317 (431)	63,200	428
8a			+181 (391)	408	-293 (435)	55,800	427
1a	Acetone	20.7	+215 (382)	397	-415 (424)	61,000	423
2a			+172 (380)	397	-333 (424)	59,700	420
8a			+182 (387)	404	-322 (430)	55,400	426
1a	Ethanol	24.3	+236 (387)	404	-413 (431)	61,800	431
2a			+164 (384)	400	-307 (428)	63,600	426
8a			+168 (389)	405	-284 (434)	55,900	426
1a	Methanol	32.6	+238 (385)	402	-408 (429)	62,600	427
2a			+154 (382)	399	-290 (426)	64,800	424
8a			+177 (386)	405	-285 (431)	56,600	425
1a	Acetonitrile	36.2	+207 (379)	395	-391 (421)	59,900	419
2a			+165 (378)	395	-318 (421)	58,100	417
8a			+181 (384)	403	-315 (429)	55,000	423
1a	N,N-Dimethylformamide	36.7	+226 (383)	399	-422 (427)	59,700	425
2a			+165 (382)	399	-317 (427)	58,400	421
8a			+165 (386)	404	-246 (429)	53,100	421
1a	Dimethylsulfoxide	46.5	+234 (383)	400	-417 (427)	59,700	426
2a			+ 83 (379)	394	-179 (421)	60,300	421
8a			-5.8 (369)	385	+23.0 (425)	55,900	425

^a From Gordon, A.J.; Ford, R.A. *The Chemist's Companion*, Wiley, NY (1972), pp 4-8.

other solvents of Table 3, and the secondary amide **2a** exhibits only moderately reduced $\Delta\epsilon$ values. These data support the $^1\text{H-NMR}$ results and appear to confirm the importance of intramolecular hydrogen bonding and ridge-tile conformations (Fig. 5) in all solvents studied. Clearly, hydrogen bonding from the propionamide residues is not easily perturbed.

CONCLUDING COMMENTS

Intramolecular hydrogen bonding between propionic acid CO_2H and dipyrinone groups is known to be a dominant, conformation stabilizing force in bilirubin and its analogs.¹⁸ The current study shows that when the propionid acid residues are replaced by primary and secondary propionamide residues, intramolecular hydrogen bonding persists in all solvents. The amide hydrogen bonding is more stable than the acid hydrogen bonding, and the effect of such hydrogen bonding is to stabilize the typical folded ridge-tile conformations (Figs. 4 and 5). The extraordinarily large bisignate CD Cotton effects observed for the amides **1a** and **2a** are a result of excited state (electric dipole) interactions, or exciton coupling, between two proximal chromophores with little orbital overlap.^{24,26} The component dipyrinone chromophores of the bichromophoric mesobilirubin have strongly allowed long-wavelength electronic transitions ($\epsilon_{410}^{\text{max}} \sim 37,000$) but only a small interchromophoric orbital overlap in the folded conformation (where the dihedral angle = 100°). They interact through resonance splitting, *i.e.*, by electrostatic interaction of the local transition moment dipoles, which are oriented along the long axis of each dipyrinone.^{4,25,26} The dipyrinone-dipyrinone intramolecular exciton splitting interaction produces two long wavelength transitions in the ordinary (UV-visible) spectrum and two corresponding bands in the CD spectrum.^{4,25,26} One band is higher in energy and one is lower in energy, with the separation dependent on the strength and relative orientation of the dipyrinone electric dipole transition moments.²⁷ When observed by UV-visible spectroscopy, the two electronic transitions overlap to give the broadened long wavelength absorption band characteristic of bilirubins. In the CD spectra, however, where the two exciton transitions are oppositely signed, bisignate CEs are typically seen as predicted by theory. Thus, in contrast to UV-visible absorption bands, which may show only slight broadening when the exciton splitting energy is small,²⁸ when two oppositely signed curves overlap in the CD, there is considerable cancellation in the region between the band centers with the net result that the *observed* bisignate CE maxima are displaced from the actual locations of the (uncombined) CD transitions which typically flank the corresponding UV-visible band(s).

EXPERIMENTAL

General Procedures. All ultraviolet-visible spectra were recorded on a Perkin Elmer Model 3840 diode array or Cary 219 spectrophotometer, and all circular dichroism (CD) spectra were recorded on a JASCO J-600 instrument. Nuclear magnetic resonance (NMR) spectra were determined on a GE QE-300 300-MHz spectrometer in CDCl_3 solvent (unless otherwise specified) and reported in δ ppm downfield from $(\text{CH}_3)_4\text{Si}$. Rotations were determined in CHCl_3 on a Perkin-Elmer model 141 polarimeter. Melting points

were determined on a Mel-Temp capillary apparatus and are uncorrected. Combustion analyses were carried out by Desert Analytics, Tucson, AZ. Analytical thin layer chromatography was carried out on J.T. Baker silica gel IB-F plates (125 μ layer). Preparative layer chromatography was carried out using 1.0 mm thickness layers of Woelm silica gel F, thin layer chromatography grade. Radial chromatography was carried out on Merck Silica gel PF-254 with CaSO₄ preparative thin layer grade, using a Chromatotron (Harrison Research, Inc., Palo Alto, CA). HPLC analyses were carried out on a Perkin-Elmer Series 4 high performance liquid chromatograph with an LC-95 UV-visible spectrophotometric detector (set at 410 nm) equipped with a Beckman-Altex ultrasphere-IP 5 μ m C-18 ODS column (25 x 0.46 cm) and a Beckman ODS precolumn (4.5 x 0.46 cm). The flow rate was 1.0 mL/minute, and the elution solvent was 0.1 M di-*n*-octylamine acetate in 5% aqueous methanol (pH 7.7, 31°C).

Spectral data were obtained in spectral grade solvents (Aldrich or Fisher). Dimethylformamide (DMF), chloroform, methanol, triethylamine (Et₃N), diphenylphosphoryl azide (DPPA), tetrachloro-1,4-benzoquinone (*p*-chloranil), acetic acid, tetrahydrofuran, 98% formic acid, dichloromethane, dimethylsulfoxide and sodium borohydride, were from Aldrich. Ammonium chloride and methylamine hydrochloride were from Matheson. Dimethylformamide was dried and distilled from barium oxide; triethylamine was dried and distilled from KOH; tetrahydrofuran was dried by distillation from lithium aluminum hydride; methanol was dried (Mg, reflux) and distilled.

(\pm)-3-[2,7,9-Trimethyl-3-ethyl-(10*H*)-dipyrrinone-8-yl]butanoic Acid [β -Methylxanthobilirubic Acid] (7). Racemic β -methylxanthobilirubic acid (β -methylXBR, 7) and both (-)-(β S)-Methylxanthobilirubic Acid (7a) and (+)-(β R)-Methylxanthobilirubic Acid (7b) were prepared by saponification of the corresponding methyl esters described previously.¹⁶

(\pm)-3-[2,7,9-Trimethyl-3-ethyl-(10*H*)-dipyrrinone-8-yl]butanamide [β -Methylxanthobilirubic Acid Amide] (5). A mixture of 633 mg (2 mmol) of racemic β -methyl-XBR (7), 20 mL of dry DMF, 139 mg (2.6 mmol) of NH₄Cl, 0.55 mL (2.6 mmol) of DPPA, 0.83 mL (6 mmol) of Et₃N was stirred under Ar for 24 h at room temperature. The mixture was poured into 400 mL of refluxing CHCl₃. After cooling it was washed with 100 mL of 1M NaOH and 4x100 mL of water, then dried (Na₂SO₄), filtered and evaporated to dryness. The remaining solid was redissolved in CHCl₃ — CH₃OH (1:1) and kept 4 h at -20°C, filtered, washed with cold CHCl₃ to yield 390 mg (50%) of β -methyl-XBR amide (5) m.p. 275-6° (decomp. without melting). It had ¹H-NMR ((CD₃)₂SO) δ : 1.07 (3H, t, J=7.6 Hz), 1.12 (3H, d, J=7.1 Hz), 1.76 (3H, s), 2.07 (3H, s), 2.21 (3H, s), 2.24 (1H, dd, J=7.3, 18.9 Hz), 2.31 (1H, dd, J=7.3, 18.9 Hz), 2.50 (2H, q, J=7.6 Hz), 3.13 (1H, sextet, J=7.3 Hz), 5.91 (1H, s), 6.65 (1H, brs), 7.23 (1 H, brs), 9.76 (1H, brs), 10.17 (1H, brs) ppm and ¹³C-NMR ((CD₃)₂SO) δ : 8.03 (q, C₂¹), 10.00 (q, C₇¹), 11.98 (q, C₉-CH₃), 14.82 (q, C₃²), 17.14 (t, C₃¹), 20.24 (q, β -CH₃), 27.04 (d, C₈¹), 42.19 (t, C₈²), 97.53 (d, C₅), 121.51 (s, C₈), 121.87 (s, C₆), 122.49 (s, C₂), 123.59 (s, C₇), 127.18 (s, C₄), 128.70 (s, C₉), 147.16 (s, C₃), 171.86 (s, C₁), 173.34 (s, C₈³) ppm.

Anal. Calcd for C₁₈H₂₅N₃O₂ (315.40): C, 68.54; H, 7.99; N, 13.32

Found: C, 68.50; H, 7.84; N, 13.10.

(+)-(β S)-Methylxanthobilirubic Acid Amide (5a). From 949 mg (3 mmol) of (β S)-methylXBR (8a), 100% e.e., were obtained 445 mg (48%) of (β S)-amide (5a) using the procedure above. It had mp 281-4°C (dec. without melting). and the same NMR data as 5 and 5b, and $[\alpha]_D^{20} +35.9$ (c 0.061, CHCl₃)

for 100% ee.

(-)-(*βR*)-Methylxanthobilirubic Acid Amide (**5b**). From 633 mg (2 mmol) of (*βR*)-methyl-XBR (**8b**), 82% e.e., were obtained 246 mg (39%) of (*βR*)-amide (**5b**) using the procedure above. It had the same NMR data as above and ¹H-NMR δ: 1.17 (3H, t, J=7.6 Hz), 1.33 (3H, d, J=7.1 Hz), 1.94 (3H, s), 2.18 (3H, s), 2.46 (3H, s), 2.55 (4H, q and dd, J_q=7.6 Hz, J_d=7.4 Hz), 3.30 (1H, dd, J=7.1, 7.4 Hz), 5.33 (1H, brs), 5.54 (1H, brs), 6.10 (1H, s), 10.17 (1H, brs), 11.05 (1H, brs) ppm.

3,17-Diethyl-2,7,13,18-tetramethyl-(21H,24H)-bilin-1,19-dione-8,12-bis-3-butanamide [*β,β'*-Dimethylmesobiliverdin-XIII α Diamide] (**3**). A mixture of 236 mg (0.75 mmol) of *β*-methyl-XBR amide (**5**), 165 mL of CH₂Cl₂, 8 mL of HCOOH, and 462 mg (1.9 mmol) *p*-chloranil was heated at reflux for 24 h. About 75 mL of solvent were removed by distillation, and reflux was continued for an additional 8 h. The mixture was kept 24 h at -20°C, filtered and washed with cold CH₂Cl₂. The cold filtrate was neutralized by slow addition of saturated aq. NaHCO₃. The organic layer was washed with 4% NaOH (3x50 mL) water (4x200 mL), then dried (Na₂SO₄). After removing the solvent the complex mixture was separated by radial chromatography (2 mm plate, 150 mL of 7.5% CH₃OH in CH₂Cl₂ and 150 mL of 10% CH₃OH in CH₂Cl₂) collecting a relatively polar pure blue band. After evaporation of the solvent and drying under vacuum, the yield was 100 mg (44%) of a mixture of (*βS, β'S*), (*βR,β'R*) and (*βS, β'R*) isomers, m.p. 149-156°C (gas evolution). It had ¹H-NMR δ: 1.14 (6H, t, J=7.4 Hz), 1.41 (6H, d, J=7.0 Hz), 1.74 (6H, deformed s), 2.13 (6H, s), 2.48 (4H, q, J=7.3 Hz), 2.56 (2H, dd, J=6.0, 13.2 Hz), 2.61 (2H, dd, J=10.4, 13.2 Hz), 3.52 (2H, sextet, J=7.5 Hz), 5.44 (1.2H, brs, racemic CONHH), 5.79 (0.8H, brs, meso CONHH), 5.90 (0.8H, s, meso H(5.15)), 5.93 (1.2 H, s, racemic H(5.15)), 6.45 (0.8 H, brs, meso CONHH), 6.75 (1.2 H, brs, racemic CONHH), 7.01 (1H, s, H(10)), 8.7-9.0 (2H, brs, H(21,24)) ppm and ¹³C-NMR δ: 8.29 (q, C₂¹, C₁₈¹), 10.34 (q, rac. C₇¹, C₁₃¹), 10.51 (q, meso C₇¹, C₁₃¹), 14.46 (q, C₃², C₁₇²), 17.82 (t, C₃¹, C₁₇¹), 20.45 (q, meso *β*-CH₃), 21.05 (q, rac. *β*-CH₃), 28.49 (d, rac. C₈¹, C₁₂¹), 28.76 (d, meso C₈¹, C₁₂¹), 43.25 (t, rac. C₈², C₁₂²), 43.46 (t, meso C₈², C₁₂²), 96.38 (d, meso C₅, C₁₅), 96.77 (d, rac. C₅, C₁₅), 115.86 (d, meso C₁₀), 116.51 (d, rac. C₁₀), 126.98 (s, meso C₈, C₁₂), 127.17 (s, rac. C₈, C₁₂), 128.22 (s, C₆, C₁₄), 139.84 (s, C₂, C₁₈), 140.17 (s, rac. C₇, C₁₃), 140.28 (s, meso C₇, C₁₃), 141.76 (s, C₄, C₁₆), 146.85 (s, C₉, C₁₁), 150.02 (s, C₃, C₁₇), 172.84 (s, C₁, C₁₉), 174.57 (s, C₈³, C₁₂³) ppm.

Anal. Calcd for C₃₅H₄₄N₆O₄ (612.78): C, 68.60; H, 7.24; N, 13.72.

Calcd for C₃₅H₄₄N₆O₄ · CH₃OH (644.82): C, 67.00; H, 7.50; N, 13.03.

Found: C, 66.61; H, 7.24; N, 12.78.

(+)-(*βS,β'S*)-Dimethylmesobiliverdin-XIII α Diamide (**3a**). Using the procedure above, 441 mg (1.4 mmol) of (*βS*)-methyl-XBR amide (**5a**), 100% e.e., was converted into 207 mg (48%) of (*βS,βS*)-verdin **3a**, mp 226-228°C. It had [α]_D²²_C+3210 (c 3.0 x 10⁻³ CHCl₃) for 100% e.e.; ¹H-NMR δ: 1.14 (6H, t, J=7.5 Hz), 1.41 (6H, d, J=7.1 Hz), 1.69 (6H, s), 2.10 (6H, s), 2.47 (4H, q, J=7.5 Hz), 2.56 (2H, dd, J=5.9, 18.0 Hz), 2.61 (2H, dd, J=10.0, 18.0 Hz), 3.52 (2H, dq, J=2.2, 7.1 Hz), 5.10 (2H, brs, CONHH), 5.89 (2H, s), 6.89 (2H, brs, CONHH), 7.02 (1H, s), 8.9-9.2 (2H, brs) ppm and ¹³C-NMR δ: 8.27 (q, C₂¹, C₁₈¹), 10.31 (q, C₇¹, C₁₃¹), 14.46 (q, C₃², C₁₇²), 17.76 (t, C₃¹, C₁₇¹), 20.90 (q, *β'*-CH₃), 28.44 (d, C₈¹, C₁₂¹), 43.20 (t, C₈², C₁₂²), 96.97 (d, C₅, C₁₅), 116.59 (d, C₁₀), 127.17 (s, C₈, C₁₂), 128.10 (s, C₆, C₁₄), 139.68 (s, C₂, C₁₈), 140.04 (s, C₇, C₁₃), 141.78 (s, C₄, C₁₆), 146.79 (s, C₉,

C₁₁), 150.11 (s, C₃, C₁₇), 173.08 (s, C₁, C₁₉), 174.63 (s, C₈³, C₁₂³) ppm.

(-)-(*βR,β'R*)-Dimethylmesobiliverdin-XIII α Diamide (3b). Using the procedure above, 158 mg (0.5 mmol) of (*βR*)-methyl-XBR amide (5b), 82% e.e., was converted into 84 mg (55%) of (*βR,βR*)-verdin 3b containing 16% meso-(*βR,β'S*) diastereomer, mp 219-224°C.

3,17-Diethyl-2,7,13,18-tetramethyl-(10*H*,22*H*,23*H*,24*H*)-bilin-1,19-dione-8,12-bis-3-butanamide [*β,β*-Dimethylmesobilirubin-XIII α Diamide] (1). (*β,β'*)-Dimethylmesobiliverdin-XIII α diamide (3) (30 mg, 50 μ mol) was dissolved in 12 mL of CH₃OH and 5 mL of dry tetrahydrofuran (both Ar saturated). The mixture was sonicated 10 min while Ar was bubbled through it until a clear solution was obtained; then 190 mg (5 mmol) of NaBH₄ were added in 4 portions over 10 min. at room temp. (~15°C). After stirring 10 min, the mixture was quenched with 35 mL of cold water, and stirring was continued for 10 min. The precipitated yellow product was filtered, washed with 4x10 mL of H₂O and dried under vacuum. The mixture of diastereoisomers was separated by radial chromatography, eluting with 3% CH₃OH and 3% acetic acid in CH₂Cl₂ to separate two bands. Both bands, after removing the solvent, were precipitated with CH₃OH to give 12 mg of "less polar" rubin-bis amide (39%) and 5 gm of "more polar" rubin-bis amide (16%). The "less polar" product had m.p. 344-352°C (decomp.); stable up to 325°C. HPLC showed the presence of racemic 1 and meso 1 in both samples (retention times: 7.86 and 6.17 minutes, respectively).

(-)-(*βS,β'S*)-Dimethylmesobilirubin-XIII α Diamide (1a). Using the same procedure as above, 61 mg (0.1 mmol) of (*βS,β'S*)-dimethylmesobiliverdin-XIII α bis-amide (3a), (100% e.e. of starting dipyrinone) gave, after crystallization from CH₃OH, 29 mg (47%) of rubin-bis-amide (1a). On HPLC it showed one peak at 7.86 min. It had m.p. 336-342° (decomp.) and [α]_D²⁰ -5770, [α]₅₇₈ -6350, [α]₅₄₆ -9120 (c 3.3 x10⁻³, CHCl₃).

(+)-(*βR,β'R*)-Dimethylmesobilirubin-XIII α Diamide (1b). Using the same procedure as above, 84 mg (138 μ mol) (*βR,β'R*)-dimethylmesobiliverdin-XIII α bis-amide (3b), (82% ee of starting dipyrinone) gave, after crystallization from CH₃OH, 43 mg (51%) of rubin-bis-amide (1b). It had m.p. 336-340° (decomp.), 98% ee (calculated); [α]_D²⁰ +5480, [α]₅₇₈ +6060, [α]₅₄₆ +8640 (c 3.5 x10⁻³, CHCl₃); UV-visible ϵ ₄₂₉^{max} 59,900 (CHCl₃), ϵ ₄₂₇^{max} 62,600 (CH₃OH), ϵ ₄₂₆^{max} 59,700 ((CH₃)₂SO); ¹H-NMR in Table 1; ¹³C-NMR δ : 8.02 (q, C₂¹, C₁₈¹), 11.03 (q, C₇¹, C₁₃¹), 14.90 (q, C₃², C₁₇²), 17.84 (t, C₃¹, C₁₇¹), 21.30 (q, *β,β'*-CH₃), 21.47 (t, C₁₀), 26.16 (d, C₈¹, C₁₂¹), 40.68 (t, C₈², C₁₂²), 98.79 (d, C₅, C₁₅), 120.90 (s, C₈, C₁₂), 122.58 (s, C₆, C₁₄), 123.11 (s, C₂, C₁₈), 124.47 (s, C₇, C₁₃), 128.11 (s, C₄, C₁₆), 132.67 (s, C₉, C₁₁), 147.75 (s, C₃, C₁₇), 174.35 (s, C₁, C₁₉), 176.85 (s, C_q³, C₁₂³) ppm.

Anal. Calcd for C₃₅H₄₆N₆O₄ (614.76): C, 68.32; H, 7.54; N, 13.67.

Found: C, 67.92; H, 7.06; N, 13.55.

(\pm)-3-[2,7,9-Trimethyl-3-ethyl-(10*H*)-dipyrinon-8-yl] N-methyl-butanamide [*β*-Methylxanthobilirubic Acid N-Methylamide] (6). A mixture of 633 mg (2 mmol) of racemic *β*-methyl-XBR (7), 677 mg (10 mmol) of methylamine hydrochloride (freshly sublimed), 1.65 g (1.27 mL, 6 mmol) of DPPA, 1.7 mL of triethylamine in 17 mL of dry DMF was stirred under Ar for 24 hours. The mixture was poured with vigorous stirring into 250 mL of water and 250 mL of CHCl₃. The water layer was extracted with 5x30 mL CHCl₃ and the combined organic extracts were washed with 3% NaOH (2x50 mL) and water (4x100

mL), then dried (Na_2SO_4). The solvent was removed under vacuum, and the crude product was recrystallized from CHCl_3 - CH_3OH to give 544 mg (83%) of β -methyl XBR-N-methylamide (**6**) m.p. 263-265°C. It had $^1\text{H-NMR}$ δ : 1.17 (3H, t, $J=7.6$), 1.31 (3H, d, $J=7.2$ Hz), 1.94 (3H, s), 2.18 (3H, s), 2.46 (3H, s), 2.47/2.48 (2H, dd, $J=2.9$, 16), 2.55 (2H, q, $J=7.6$ Hz), 2.71/2.73 (3H, s), 3.31 (1H, sextet, $J=7.3$ Hz), 5.26/5.27 (1H, s), 6.13 (1H, s), 10.27 (1H, brs), 11.23 (1H, brs) ppm; $^1\text{H-NMR}$ ($(\text{CD}_3)_2\text{SO}$) δ : 1.04 (3H, t, $J=7.6$ Hz), 1.07 (3H, d, $J=7.3$ Hz), 1.73 (3H, s), 2.03 (3H, s), 2.17 (3H, s), 2.21 (1H, dd, $J=8.4$, 13.8 Hz), 2.30 (1H, dd, $J=6.9$, 13.8 Hz), 2.47 (2H, q, $J=7.6$ Hz), 2.47/2.49 (3H, s), 3.11 (1H, sextet, $J=7.3$ Hz), 5.88 (1H, s), 7.66/7.67 (1H, s), 9.74 (1H, s), 10.14 (1H, s) ppm; $^{13}\text{C-NMR}$ δ : 8.04 (q, C_2^1), 10.00 (q, C_7^1), 11.98 (q, C_9 - CH_3), 14.84 (q, C_3^2), 17.14 (t, C_3^1), 20.16 (q, β - CH_3), 25.36 (q, NCH_3), 27.14 (d, C_8^1), 42.44 (t, C_8^2), 97.53 (d, C_5), 121.52 (s, C_8), 121.82 (s, C_6), 122.52 (s, C_2), 123.56 (s, C_7), 127.20 (s, C_4), 128.66 (s, C_9), 147.18 (s, C_3), 171.59 (s, C_8^3), 171.87 (s, C_1) ppm.

(+)-(βS)-Methylxanthobilirubic acid N-methylamide (**6a**). As described above, 948 mg (3 mmol) of (βS)-methyl XBR (**8a**), 100% e.e., gave 856 mg (87%) of N-methylamide **6a**. It had m.p. 249-250°C and the same NMR as **6** and $[\alpha]_{\text{D}}^{20} +62.8^\circ$ (c 0.078, CHCl_3) for 100% e.e.

Anal. Calcd for $\text{C}_{19}\text{H}_{27}\text{N}_3\text{O}_2$ (329.43): C, 69.27; H, 8.26; N, 12.76.

Found: C, 69.65; H, 8.01; N, 12.67.

3,17-Diethyl-2,7,13,18-tetramethyl-(21H,24H)-bilin-1,19-dione-8,12-bis-3-(N-methyl)butanamide [β,β' -Dimethylmesobiliverdin-XIII α Bis-N-methylamide] (4**)**. A mixture of 329 mg (1 mmol) of racemic β -methyl-XBR N-methylamide (**6**) (616 mg, 2.5 mmol), *p*-chloranil, 220 mL of CH_2Cl_2 , and 10 mL 97% HCOOH was heated at reflux for 24 hours. One hundred and ten milliliters were removed by distillation and reflux was continued for 4 hours more. The mixture was kept 20 h at -20°C and filtered. The filtrate was neutralized cold with saturated aq. NaHCO_3 . The organic layer was washed with 4% NaOH (3x30 mL), water (5x100 mL), dried with Na_2SO_4 and evaporated to dryness. The crude product was purified by radial chromatography (2 mm plate, 6% $\text{CH}_3\text{OH-CH}_2\text{Cl}_2$) to give 202 mg (63%) of pure verdin, m.p. 246-8°C (decomp.). It had $^1\text{H-NMR}$ δ : 1.21 (6H, t, $J=7.6$ Hz), 1.47 (6H, d, $J=7.2$ Hz), 1.82 (6H, s), 2.16 (6H, s), 2.49 (4H, dd), 2.52 (4H, q, $J=7.6$ Hz), 2.70 (6H, d, $J=4.7$ Hz), 3.54 (2H, sextet, $J=7.3$ Hz), 5.96 (2H, s), 6.37 (2H, brq, $J=4.7$ Hz), 7.08 (1H, s), 8.37 (2H, brs) ppm; $^{13}\text{C-NMR}$ δ : 8.30 (q, C_2^1 , C_{18}^1), 10.46 (q, C_7^1 , C_{13}^1), 14.45 (q, C_3^2 , C_{17}^2), 17.86 (t, C_3^1 , C_{17}^1), 20.17 (q, β - CH_3), 26.46 (q, NCH_3), 29.09 (d, C_8^1 , C_{12}^1), 44.59 (t, C_8^2 , C_{12}^2), 96.34 (d, C_5 , C_{15}), 115.78 (d, C_{10}), 126.94 (s, C_8 , C_{12}), 128.25 (s, C_6 , C_{14}), 139.82 (s, C_2 , C_{18}), 140.36 (s, C_7 , C_{13}), 142.04 (s, C_4 , C_{16}), 146.89 (s, C_9 , C_{11}), 150.11 (s, C_3 , C_{17}), 172.51 (s, C_1 , C_{19}), 172.57 (s, C_8^3 , C_{12}^3) ppm.

Anal. Calcd for $\text{C}_{37}\text{H}_{48}\text{N}_6\text{O}_4$ (640.80): C, 69.35; H, 7.55; N, 13.12.

Found: C, 69.30; H, 7.18; N, 12.77.

(+)-($\beta\text{S},\beta\text{S}$)-Dimethylmesobiliverdin-XIII α Bis-N-methylamide (**4a**). As described above, 659 mg (2 mmol) of (βS)-methyl-XBR N-methylamide (**6a**), 100% ee, was converted into 371 mg (58%) of verdin **4a**, mp 264-268°C (dec.). It had mp 264-266°C, the same NMR as **4**, and $[\alpha]_{\text{D}}^{20} +1050^\circ$ (c 3.0 $\times 10^{-3}$, CHCl_3) for 100% e.e.

3,17-Diethyl-2,7,13,18-tetramethyl-(10H,22H,23H,24H)-bilin-1,19-dione-8,12-bis-3-(N-methyl)butanamide [β,β' -Dimethylmesobilirubin-XIII α Bis-N-methylamide] (2**)**. β,β' -dimethylmesobiliver-

din-XIII α bis-N-methylamide (4) (143 mg, 0.22 mmol) was dissolved in 40 mL of dry, N₂-saturated tetrahydrofuran. Under N₂, NaBH₄ (836 mg, 22 mmol) was added followed by 20 mL of dry methanol over 15 min. The yellow solution was quenched with 200 mL of water and acidified at 0°C with 10% HCl. The product was extracted with CHCl₃ (5x40 mL), washed with water (3x100 mL), dried (Na₂SO₄) and evaporated to dryness. On TLC (SiO₂, 5% CH₃OH in CHCl₃) two spots of the polar crude product were hardly separated. The crude solid was stirred with 5 mL of CHCl₃, filtered and washed with CHCl₃ to yield 115 mg (80%) of rubins. Two peaks were detected by HPLC with retention times: 4.33 min (meso) and 4.55 min (racemic) in a ratio 30:70. The unseparated product had m.p. 294–8°C (decom.).

(-)-(βS,β'S)-Dimethylmesobilirubin-XIII α Bis-N-methylamide (2a). Using the same procedure above, 141 mg of βS,β'S-dimethyl mesobiliverdin-XIII α bis-N-methylamide (4a) (100% ee) gave 92 mg (65%) (from 2 mL of CH₃OH and 5 mL of CHCl₃) of optically active rubin 2a with m.p. 298–302°C (decomp.). On HPLC it showed one peak at 4.55 min (coinjection of this sample of 2a with the sample from above showed again two peaks: retention time 4.33, 4.55 min). It had $[\alpha]_D^{20}$ -5180, $[\alpha]_{578}$ -5740, $[\alpha]_{546}$ -8220 (*c* 4.4 x 10⁻³, CHCl₃); UV-visible ϵ_{428}^{\max} 57,600 (CHCl₃), ϵ_{424}^{\max} 64,800 (CH₃OH), ϵ_{421}^{\max} 60,300 ((CH₃)₂SO); ¹H-NMR in Table 1, ¹³C-NMR δ : 8.12 (q, C₂¹, C₁₈¹), 11.14 (q, C₇¹, C₁₃¹), 14.96 (q, C₃², C₁₇²), 17.84 (t, C₃¹, C₁₇¹), 21.53 (t, C₁₀), 21.88 (q, ββ'-CH₃), 25.80 (q, NCH₃), 28.85 (d, C₈¹, C₁₂¹), 37.60 (t, C₈², C₁₂²), 98.80 (d, C₅, C₁₅), 120.69 (s, C₈, C₁₂), 122.91 (s, C₆, C₁₄), 122.96 (s, C₂, C₁₈), 124.33 (s, C₇, C₁₃), 127.92 (s, C₄, C₁₆), 132.84 (s, C₉, C₁₁), 147.73 (s, C₃, C₁₇), 174.45 (s, C₁, C₁₉), 176.59 (s, C₈³, C₁₂³) ppm.

Anal. Calcd for C₃₇H₅₀N₆O₄ (642.81): C, 69.13; H, 7.84; N, 13.07.

Found: C, 68.63; H, 7.50; N, 12.37.

Molecular Dynamics. Molecular mechanics calculations and molecular modelling was carried out on an Evans and Sutherland ESV-10 workstation using version 5.41 of SYBYL (Tripos Assoc., St. Louis, MO). The dipyrinone units of bilirubin, β,β-dimethylmesobilirubin-XIII and its bis-amides were rotated independently about the central -CH₂- at C₁₀ (torsion angles ϕ_1 and ϕ_2) through 10° increments from 0° to 360°. (The $\phi_1=0^\circ$, $\phi_2=0^\circ$ conformer has a porphyrin shape.) In this procedure, the two torsion angles were held fixed at each increment while the remainder of the molecule was relaxed to its minimum energy conformation using molecular mechanics. This was followed by a molecular dynamics cooling curve consisting of the following temperatures and times: 100 fs at 20°K, 100 fs at 10°K, 100 fs at 5°K, 200 fs at 2°K, 200 fs at 1°K, 200 fs at 0.5°K, 300 fs at 0.1°K. This was followed by molecular mechanics minimization, which gave the lowest energy conformations for each set of ϕ values. The conformational energy maps were created using Wingz™ (Informix), and the ball and stick drawings were created from the atomic coordinates of the molecular dynamics structures using Müller and Falk's "Ball and Stick" program (Cherwell Scientific, Oxford, U.K.) for the Macintosh.

Acknowledgement. We thank the National Institutes of Health (HD 17779) for generous support of this work. Dr. S.E. Boiadjev is on leave from the Institute of Organic Chemistry, Bulgarian Academy of Sciences. Mr. R.V. Person gratefully acknowledges awards of an R.C. Fuson Graduate Fellowship and the Wilson Graduate Fellowship. We thank Mr. Lew Cary for invaluable assistance in obtaining NOE data for the ¹H-NMR spectra.

REFERENCES

- (1) Gollan, J. (Guest ed.) *Seminars in Liver Disease* 1988, 8, 103-199, 272-283.
- (2) For leading references, see Ostrow, J. D., Ed. *Bile Pigments and Jaundice*; Marcel-Dekker: New York, 1986.
- (3) Falk, H. *The Chemistry of Linear Oligopyrroles and Bile Pigments*; Springer Verlag: New York, 1989.
- (4) Lightner, D.A.; Person, R.V.; Peterson, B.R.; Puzicha, G.; Pu, Y.-M.; Bojadziej, S. *Biomolecular Spectroscopy II* (Birge, R.R.; Nafie, L.A., eds.), Proc. SPIE 1432, 1991, 2-13.
- (5) Falk, H.; Müller, N. *Tetrahedron* 1983, 39, 1875-1885.
- (6) Molecular mechanics calculations indicate a global minimum for the (folded) conformation with $\phi_1 \approx \phi_2 \approx 62^\circ$ (where ϕ_1 and ϕ_2 are defined as 0° in the porphyrin-like conformation). Intramolecular hydrogen bonding is computed to lower the total energy of the folded conformation by an additional 16 kcal/mole. (Refs. 3, 4 and 5)
- (7) (a) Bonnett, R.; Davies, J. E.; Hursthouse, M. B.; Sheldrick, G. M. *Proc. R. Soc. London, Ser. B* 1978, 202, 249-268.
(b) LeBas, G.; Allegret, A.; Mauguén, Y.; DeRango, C.; Bailly, M. *Acta Crystallogr., Sect. B* 1980, B36, 3007-3011.
(c) Becker, W.; Sheldrick, W. S. *Acta Crystallogr., Sect. B* 1978, B34, 1298-1304.
- (8) Mugnoli, A.; Manitto, P.; Monti, D. *Acta Crystallogr., Sect. C* 1983, 38, 1287-1291.
- (9) (a) Kaplan, D.; Navon, G. *Isr. J. Chem.* 1983, 23, 177-186.
(b) Kaplan, D.; Navon, G. *Org. Magn. Res.*, 1981, 17, 79-87.
(c) Kaplan, D.; Navon, G. *Biochem. J.* 1982, 201, 605-613.
(d) Navon, G.; Frank, S.; Kaplan, D. *J. Chem. Soc. Perkin Trans. 2* 1984, 1145-1149.
- (10) Manitto, P.; Monti, D. *J. C. S. Chem. Commun.* 1976, 122-123.
- (11) Puzicha, G.; Pu, Y.M.; Lightner, D.A. *J. Am. Chem. Soc.* 1991, 113, 3583-3592.
- (12) Trull, F.R.; Franklin, R.W.; Lightner, D.A. *J. Heterocyclic Chem.* 1987, 24, 1573-1579.
- (13) Blanckaert, N.; Heirwegh, K.P.M.; Zaman, Z. *Biochem. J.* 1977, 164, 229-236.
- (14) McDonagh, A.F.; Lightner, D.A. In *Hepatic Metabolism and Disposition of Endo and Xenobiotics* (Falk Symposium No. 57, Bock, K.W.; Gerok, W.; Matern, S., eds.) Kluwer, Dordrecht, The Netherlands, 1991, Chap. 5, pp 47-59.
- (15) (a) Lightner, D.A.; McDonagh, A.F. *Accounts Chem. Res.* 1984, 17, 417-424.
(b) McDonagh, A.F.; Lightner, D.A. *Pediatrics* 1985, 75, 443-455.
- (16) Boiadjiev, S.E.; Person, R.V.; Lightner, D.A. *J. Am. Chem. Soc.* 1992, 114, 10123-10133.
- (17) Shioiri, T.; Ninomiya, K.; Yamada, S. *J. Am. Chem. Soc.* 1972, 94, 6203-6205.
- (18) Lightner, D.A.; Ma, J.-S.; Adams, T.C.; Franklin, R.W.; Landen, G.L. *J. Heterocyclic Chem.* 1984, 21, 139-144.
- (19) Lightner, D.A.; Adams, T.C.; Ma, J.-S. *Tetrahedron* 1984, 40, 4253-4260.
- (20) Shrout, D.P.; Puzicha, G.; Lightner, D.A. *Synthesis* 1992, 328-332.
- (21) Trull, F.R.; Ma, J.S.; Landen, G.L.; Lightner, D.A. *Isr. J. Chem.* 1983, 23, 211-218.
- (22) Puzicha, G.; Pu, Y.-M.; Lightner, D.A. *J. Am. Chem. Soc.* 1991, 113, 3583-3592.
- (23) Gawroński, J.K.; Pofonski, T. and Lightner, D.A. *Tetrahedron* 1990, 46, 8053-8066.
- (24) Harada, N.; Nakanishi, K. *Circular Dichroic Spectroscopy - Exciton Coupling in Organic Stereochemistry*; University Science Books: Mill Valley, CA, 1983.
- (25) Lightner, D.A.; Gawroński, J.; Wijekoon, W.M.D. *J. Am. Chem. Soc.* 1987, 109, 6354-6362.
- (26) Person, R.V.; Boiadjiev, S.E.; Peterson, B.R.; Puzicha, G.; Lightner, D.A. "4th International Conference on Circular Dichroism," Sept. 9-13, 1991, Bochum, FRG, pp 55-74.
- (27) Blauer, G.; Wagnière, G. *J. Am. Chem. Soc.* 1975, 97, 1949-1954.
- (28) Kasha, M.; Rawls, H.R.; El-Bayoumi, M.A. *Pure Appl. Chem.* 1965, 32, 371-392.